Polskie Towarzystwo Materiałów Kompozytowych
Polish Society of Composite Materials

25: 4 (2025) 234–242

COMPOSITES THEORY AND PRACTICE

ISSN (online): 2299-128X

Paulina Kozera*, Łukasz Sarniak, Kamil Dydek, Andrzej Wolanin, Anna Boczkowska

Faculty of Materials Science and Engineering, Warsaw University of Technology, 141 Wołoska St., 02-507 Warsaw, Poland

* *Correspondence:* paulina.kozera@pw.edu.pl

Received (Otrzymano) 5.10.2025
Published on-line (Opublikowano) 31.12.2025

DEVELOPMENT OF ULTRASONIC TECHNIQUE USING PHASED ARRAY PROBES IN TYPE IV LOW-PRESSURE TANK

https://doi.org/10.62753/ctp.2025.04.4.4

The aim of this work is to develop an ultrasonic technique employing phased array probes to detect structural defects in type IV low-pressure tanks used for the storage of hazardous chemicals. Ultrasonic testing was performed by means of an OmniScan MX2 phased-array ultrasonic flaw detector with appropriate probes, and numerical simulations were conducted utilizing CIVA software. Attenuation coefficients were measured for a composite layer excised from a two-layer low-pressure tank. Based on these results, a centre frequency of 5 MHz was selected as optimal. The determined parameters, such as the attenuation coefficient and the structural noise level, were implemented in the CIVA model. The detection criteria were established and color-coded: defects with a signal-to-noise ratio (SNR) < 0 dB were labelled white (undetectable); those 0–10 dB were labelled yellow (limited detectability); and those > 10 dB were labelled green (optimal detectability). The simulation results were validated by testing the composite samples with polytetrafluoroethylene (PTFE) inserts of varying sizes and depths. The defect detectability determined from the simulations was consistent with that obtained from testing reference samples.

Keywords: ultrasonic testing, phased array, attenuation, delamination, defects, composite tank, liner, GFRP, numerical simulations

INTRODUCTION

Ultrasonic testing (UT) uses ultrasonic waves in the frequency range from several kilohertz (kHz) to several megahertz (MHz) to evaluate materials and their internal structure. The measurement of ultrasonic wave attenuation is important for defect detection analysis. The energy of an ultrasonic wave passing through the test material is reduced due to:

- the absorption of ultrasonic wave energy because of the internal friction of vibrating particles; mechanical energy is converted into thermal energy
- reflection, refraction, diffraction, and dispersion, which occur mainly in inhomogeneous and polycrystalline media with an imperfect structure. For example, an ultrasonic wave can be reflected from individual structural defects, including grain boundaries in a non-homogeneous material [1].

In real elastic media, ultrasonic waves are significantly attenuated. Their energy decreases and, consequently, the acoustic pressure is reduced. Wave attenuation arises from structural and geometric factors. The former produces specific attenuation, associated with the absorption of ultrasonic energy, i.e. irreversible energy transfer processes and the conversion of mechanical energy into heat. This type of attenuation occurs in all states of matter. In solid media, energy absorption is caused by the nonlinear dependence of strain on

stress. Structural attenuation arises from interactions between the wave and the material microstructure, as well as with other waves [2].

The influence of individual mechanisms depends on the vibration frequency. Dislocation attenuation occurs at low frequencies, whereas interactions of elastic waves with conduction electrons occur at high frequencies. In polycrystalline solids, attenuation is generally considered to result from the combined action of various absorption mechanisms [3, 4].

Geometric factors – often termed attenuation by dispersion – occur mainly in inhomogeneous or polycrystalline materials. These arise from interactions with internal boundaries, as well as from ultrasonic-beam divergence. As energy is redistributed, only a portion reaches the receiving transducer, observed as a pressure drop.

For metals and their alloys, polycrystalline inhomogeneity with respect to ultrasonic-wave propagation results from the random orientation of grains. Because individual grains are anisotropic, the wave velocity changes upon crossing a grain boundary. Greater anisotropy generally leads to greater attenuation. However, this type of attenuation is strongly influenced by the ratio of the wavelength to the average grain diameter. Energy dispersion is also caused by defects such as non-metallic inclusions, cracks, pores, and voids [5–8].

For composite materials, an ultrasonic wave is attenuated by scattering, absorption, and beam divergence. Attenuation depends on its wavelength, and scattering is influenced by features larger than ~0.1 of the wavelength. Defects smaller than ~0.5 wavelength are generally not detectable by ultrasonic testing [9]. Hence, the actual attenuation depends on many factors, such as the fibre properties, matrix properties, and fibre arrangement in the matrix.

Attenuation coefficient α characterizes the attenuation of the medium. The total attenuation coefficient can be expressed as:

$$\alpha = \alpha 1 + \alpha 2 \tag{1}$$

where: α1 – absorption coefficient, α2 – scattering coefficient.

The measurement of wave attenuation is used to determine key features of the microstructure of materials to support their classification, and to assess the current degree of wear of materials operating under harsh service conditions.

Because type IV low-pressure tanks can exhibit various failure modes, such as fatigue, stress rupture, and burst due to over-pressurization or damage, it is important to inspect them using non-destructive testing (NDT). Currently, several established techniques – such as thermography, shearography, radiography, and acoustic emission testing [10] – have been shown to produce meaningful results reliably. Nevertheless, whether ultrasonic testing (UT) can also serve as an effective additional diagnostic tool remains an open question. UT of composite structures (particularly glass fiber reinforced polymer, GFRP) poses major challenges to metals, including pronounced signal attenuation, direction dependent wave velocities, and strong reflections at fabric-resin interfaces [11]. Research is increasingly focusing on understanding the complex interaction between ultrasound and laminate components to obtain detailed 3D characterization [12, 13]. The anisotropic nature of composites introduces beam skew, complicating precise defect sizing and accurate localization during UT-based evaluation. In addition to anisotropy, the complexity is further increased by the intricate geometries that these materials often possess. Phased array ultrasonic testing (PAUT) addresses the limitations of conventional UT by enabling electronic focusing and steering to target specific angles and locations [14]. Given the complex construction of type IV low-pressure composite tanks, PAUT appears to be well-suited for diagnosing defects in their composite structure.

This study investigates the effect of the ultrasonic wave frequency on the attenuation coefficient value, and depths of artificial defects on their detectability in the GFRP sample cut out of a type IV low-pressure tank. Practical tests were supported by numerical simulations using CIVA software. Based on the signal-to-noise ratio (SNR), the detection criteria were established. The re-

ceived results in this study may develop the ultrasonic technique using phased array probes in type IV low-pressure tanks.

MATERIALS

Ultrasonic wave attenuation measurements were conducted on composite samples cut from the double-layer wall of low-pressure tanks. The tank shown in Figure 1 was manufactured using filament winding equipment (Mikrosam, Prilep, Macedonia) at Amargo. The tank was fabricated by the filament winding of continuous resin impregnated glass roving onto a thermoplastic liner. The tank (2 m in height and 0.7 m in diameter) consisted of two layers: GFRP and PE. The GFRP was manufactured using SE1200 single-end Type 30™ glass fiber roving from Owens Corning Composite Materials (Toledo, OH, USA). The Araldite® LY 1564 / Aradur® 3486 epoxy resin system (Huntsman, Woodlands, Texas, USA) was used as the polymer matrix. Polyethylene sheets (Röchling SE & Co. KG, Mannheim, Germany) were used as the tank's second layer and as the thermoplastic liner. The thickness of the investigated GFRP layer was 1.5 mm in the first tank and 3 mm in the second.

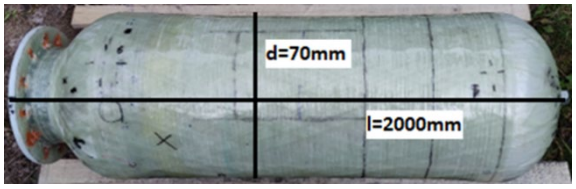

Fig. 1. Composite tank manufactured by filament winding technique

Flaw detection was evaluated on flat samples replicating the structure of a composite tank wall. For this purpose, two-layer flat samples were fabricated, with artificial flaws introduced into the composite layer in the form of polytetrafluoroethylene (PTFE) inserts measuring 5 × 5 mm, 10 × 10 mm, and 20 × 20 mm. The flaws were introduced at different sample depths: 1 mm, 2 mm, and 3 mm, as shown in Figure 2.

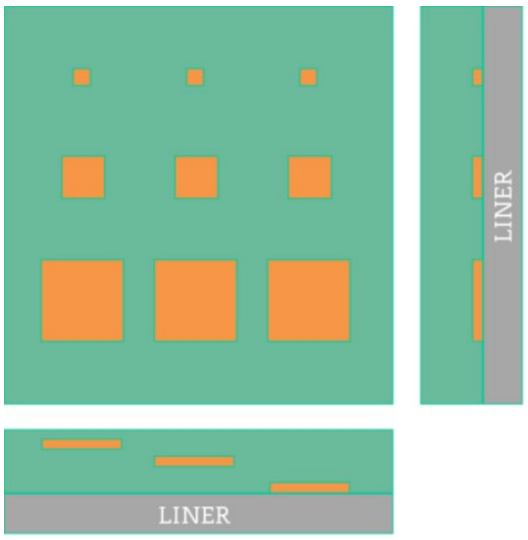

Fig. 2. Schematic diagram of arrangement of PTFE inserts in flat double-walled sample

The sample consisted of a 5 mm thick layer of glass fiber reinforced polymer (GFRP) and an additional 5 mm thick polyethylene (PE) layer. The GFRP was fabricated using unidirectional glass fiber fabric with universal sizing and an areal weight of 500 g/m² (GRM Systems, Olomouc, Czech Republic), in combination with the Araldite® LY 1564 / Aradur® 3486 epoxy resin system. Twelve plies, each measuring 400 mm × 300 mm, were laid up by the hand lay-up method at ambient temperature. The laminate, shown in Figure 3, was then post cured at 80°C for 8 h. Subsequently, a polyethylene layer (Röchling SE & Co. KG, Mannheim, Germany) was bonded to the GFRP surface using the same epoxy resin system.

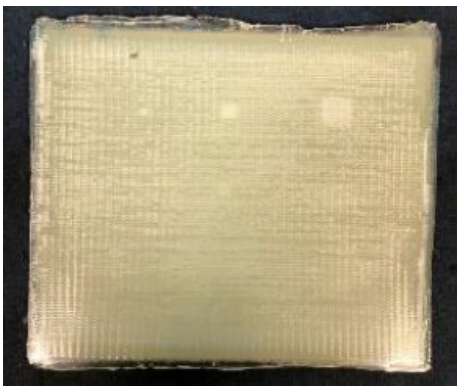

Fig. 3. Photograph of arrangement of PTFE inserts in flat double-walled sample

METHODS

Ultrasonic testing was conducted using an OmniScan MX2 ultrasonic flaw detector with a phased array system (EVIDENT Europe GmbH, Hamburg, Germany) in addition to conventional and phased array (multi-element) probes (EVIDENT Europe GmbH, Hamburg, Germany). Attenuation was measured by through-transmission (single pass) of the researched composite material of two thicknesses, 1.5 mm and 3 mm (Figure 2b). The tests were carried out using ultrasonic probes at centre frequencies of 2, 4, and 5 MHz. A schematic illustration of the ultrasonic wave attenuation measurement is shown in Figure 4. Each time, the receiver gain of the ultrasonic flaw detector was adjusted to set the transmitted signal to 80% full screen height (FSH).

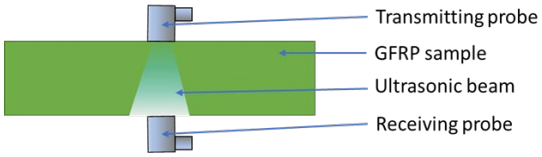

Fig. 4. Schematic visualization of ultrasonic wave attenuation measurement

The ultrasonic wave attenuation coefficients for the studied composite material were determined for three different frequencies using the formula:

$$\alpha\ [\mathrm{dB/mm}] = (G_2\ [\mathrm{dB}] - G_1\ [\mathrm{dB}]) / (t_2\ [\mathrm{mm}] - t_1\ [\mathrm{mm}]), \quad (2)$$

where G_1 and G_2 are the recorded gains for thicknesses t_1 and t_2, respectively. This is equivalent to:

$$\alpha\ [\mathrm{dB/mm}] = 20\ \log_{10}(A1 / A2) / (t_2\ [\mathrm{mm}] - t_1\ [\mathrm{mm}]), \quad (3)$$

where A_1 and A_2 are the measured peak-to-peak amplitudes (relative units) for thicknesses t_1 and t_2, respectively.

The measurements were repeated and averaged to reduce coupling variability. The ultrasonic wave attenuation coefficients for the investigated material were validated using the CIVA numerical simulation platform (CEA-List, Paris, France). The resulting attenuation coefficient values were then used in numerical simulations of ultrasonic testing in CIVA. Models of the sample and the phased array probe were employed to simulate ultrasonic wave propagation in the sample and its interaction with the defect models. Defects measuring 5 × 5 mm, 10 × 10 mm, and 20 × 20 mm were modelled at sample depths of 0.5, 1.0, 1.5, 2.0, 2.5, and 3.0 mm. A 5 MHz phased array probe model was utilized for these simulations. The signal-to-noise ratio (SNR) was determined.

RESULTS

Attenuation measurements are used to determine key microstructural features of materials, to support their classification, and to continuously assess the degree of wear of materials operating under harsh conditions. The attenuation in glass/epoxy composites is much higher than in metals or carbon fiber reinforced polymer (CFRP) composites. In general, the ultrasonic testing of materials focuses on determining the amplitude of the backwall echo (reflection from the far surface). Owing to the small thickness of the composite samples, their scattering microstructure, and surface roughness, backwall echo attenuation measurements were limited. Therefore, attenuation was measured by through-transmission (single pass) of the studied material. The results are presented in Table 1.

TABLE 1. **Dependence of attenuation coefficient on ultrasonic wave frequency in composite sample**

Sample	Thickness of composite sample t [mm]	Receiver gain of ultrasonic flaw detector was measured for transition signal at 80% FSH [dB]		
		2 MHz	4 MHz	5 MHz
1	3	42.4	48.2	49.0
2	1.5	37.7	38.0	37.0
Difference	**1.5**	**4.7**	**10.2**	**12.0**
Attenuation coefficient [dB/mm]		3.13	6.80	8.00

In the next stage, the attenuation coefficients were validated by means of the CIVA numerical simulation platform with the same frequencies: 2, 4, and 5 MHz. The verification for the researched composite material showed that the experimentally determined values were consistent with the numerical model using the implemented parameters (Table 2). The model was calibrated with the measured attenuation coefficient at 2 MHz, and the software was then employed to simulate and compute the attenuation coefficients for 4 and 5 MHz. Therefore, the adopted research methodology was validated, and the determined parameters can be used in further work.

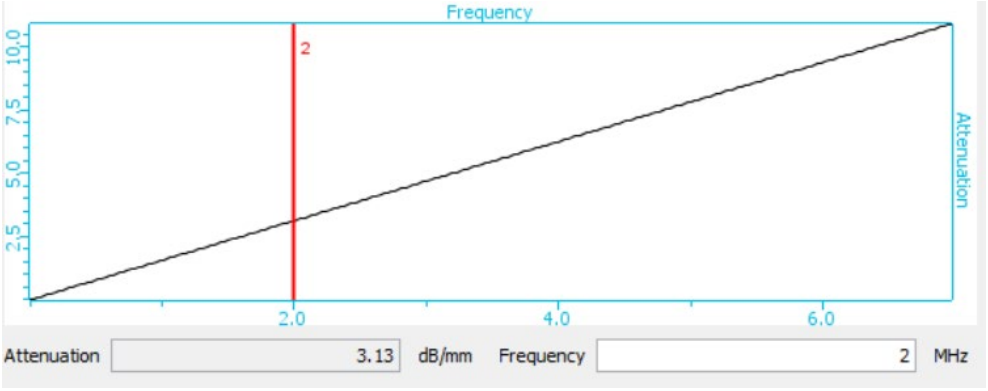

a)

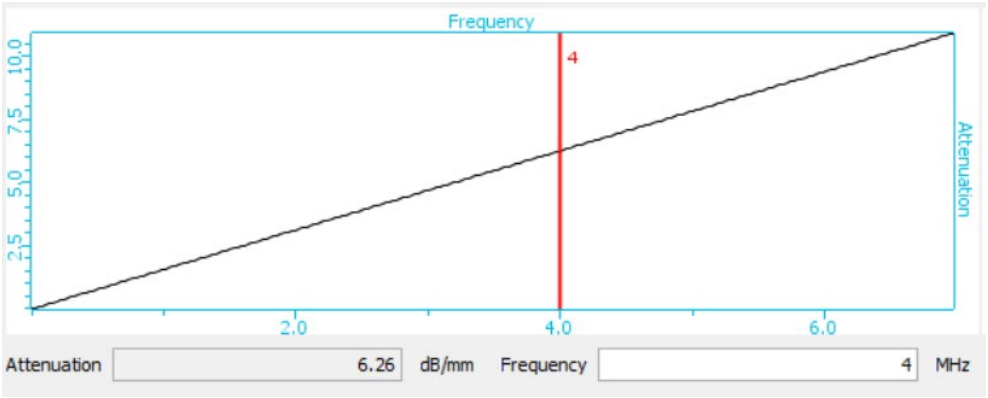

b)

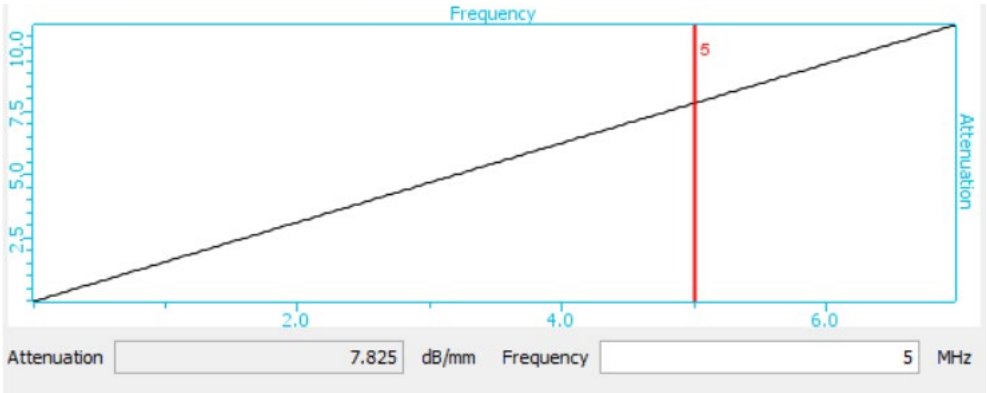

c)

Fig. 5. Verification of attenuation coefficient for studied composite material using CIVA software and a) 2 MHz, b) 4 MHz, and c) 5 MHz, respectively

TABLE 2. **Comparison of attenuation coefficient measured experimentally on sample and determined by CIVA software simulation**

Ultrasonic wave frequency	2 MHz	4 MHz	5 MHz
Attenuation coefficient measured on composite sample [dB/mm]	3.13	6.80	8.00
Attenuation coefficient determined in CIVA program [dB/mm]	3.13	6.26	7.83

The measured attenuation coefficient values were incorporated into the numerical simulations of ultrasonic tests performed in CIVA. Figure 6 shows a diagram of the sample model and the phased array probe model. For subsequent investigations, the centre frequency of 5 MHz was selected as it offered the best compromise between signal attenuation and resolution owing to its shorter wavelength. Moreover, the shorter pulse length reduced the dead zone, which is particularly important for relatively thin composite specimens and enabled reliable detection of near-surface defects.

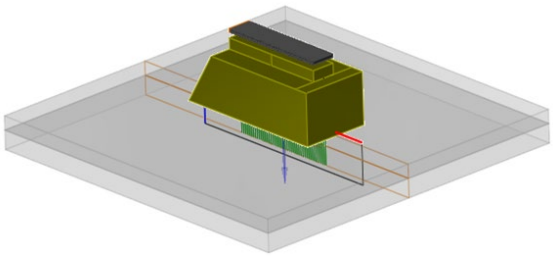

Fig. 6. Diagram of sample model and phased array probe model.

Numerical simulations were conducted to analyse the ultrasonic wave propagation in the investigated component and its interaction with the defect models. The following defects were modelled: 5 x 5 mm, 10 x 10 mm, and 20 x 20 mm, located at sample depths of 0.5 mm, 1mm, 1.5 mm, 2 mm, 2.5 mm, and 3 mm. The test results for the defect measuring 20 x 20 mm, located at depths of 1 mm, 2 mm and 3 mm, obtained utilizing a phased array probe with a frequency of 5 MHz, are presented in Figure 7.

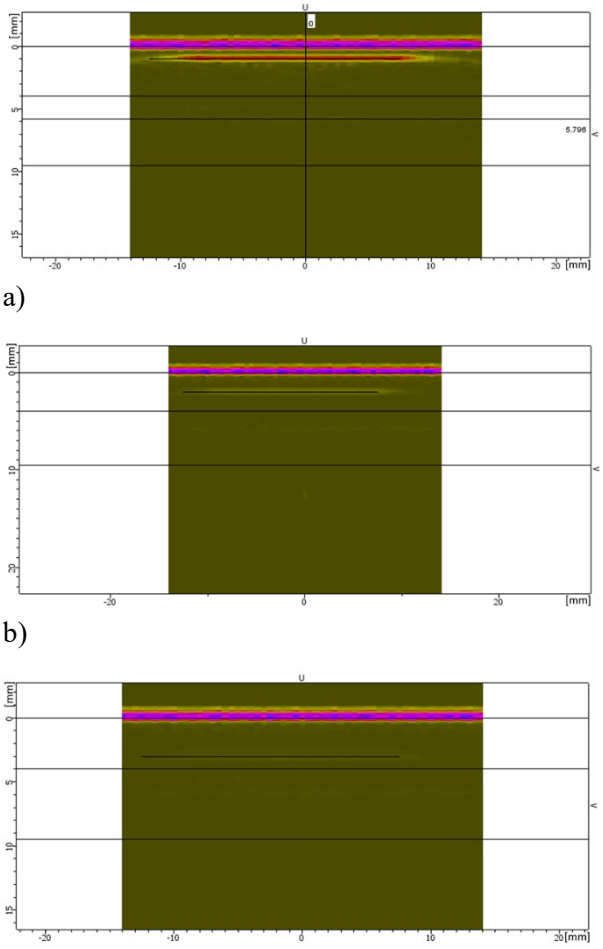

Fig. 7. Simulation of ultrasonic beam interaction of 5 MHz phased array probe (B-Scan) with delamination defect 20 x 20 mm, located at depths of 1 mm, 2 mm and 3 mm, respectively

A series of simulations was carried out to compare the amplitude of the ultrasonic wave reflected from a delamination-type discontinuity as a function of its size and depth. The level of structural noise in the composite layer was measured experimentally on reference samples, reaching an average of ~6 dB relative to the liner backwall echo. This value was incorporated into CIVA, enabling analysis of defect detectability as a function of size and depth. The signal-to-noise ratio (SNR) was

determined. An SNR of 0 means that the amplitude of the defect echo equals that of the structural noise echo, making the two indistinguishable. For SNR < 0, the defects were considered not detectable. An SNR of 10 dB indicates that the amplitude of the defect echo is approximately three times the structural noise amplitude. It was assumed that if the amplitude of the defect echo exceeds the structural noise level but is less than three times this level, defect detectability is limited. In this context, the following criteria were used: SNR > 10 dB provides optimal detectability; 0 < SNR ≤ 10 dB indicates limited detectability; and SNR < 0 prevents detection. The analyses showed that SNR varies with measurement frequency, defect size, and depth of location. The determined SNR values are presented in Table 3. Defects with SNR < 0 are marked in white as not detectable; those 0–10 dB are marked in yellow as difficult to detect, and those > 10 dB are marked in green as optimally detectable.

TABLE 3. **Comparison of signal-to-noise ratio (SNR) for delamination defects with dimensions of 5 x 5 mm, 10 x 10 mm and 20 x 20 mm for 5 MHz phased array probe depending on location depth**

Size of defect/ Location depth [mm]	SNR [dB]		
	5 x 5 mm	10 x 10 mm	20 x 20 mm
0.5	24.49	25.23	26.19
1	12.61	14.78	12.95
1.5	0.52	2.17	2.46
2	-11.58	-9.88	-10.06
2.5	-21.04	-21.04	-20.81
3	-32.77	-29.98	-30.83

Ultrasonic testing was then performed on reference samples with composite inserts measuring 5 x 5 mm, 10 x 10 mm, and 20 x 20 mm, embedded at depths of 1 mm, 2 mm, and 3 mm. The tests showed that at the frequency of 5 MHz, defects measuring 5 x 5 mm, 10 x 10 mm, and 20 x 20 mm are visible only at the depth of 1 mm. At deeper levels, these inserts are not visible, which is consistent with the results of the numerical simulations. A-, B-, and C-scans for the sample with defects measuring 5 x 5 mm, 10 x 10 mm, and 20 x 20 mm at the depth of 1 mm, compared to A, B, and C-scans for the sample with defects measuring 5 x 5 mm, 10 x 10 mm, and 20 x 20 mm at the depth of 2 mm, are shown in Figures 8 and 9.

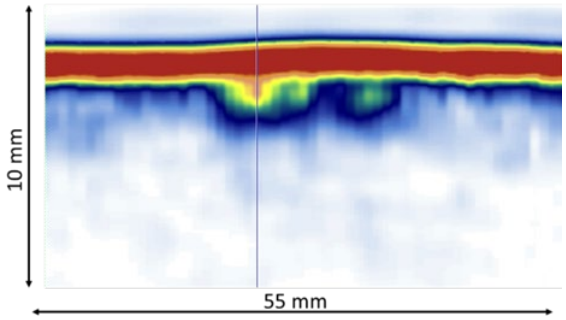

a)

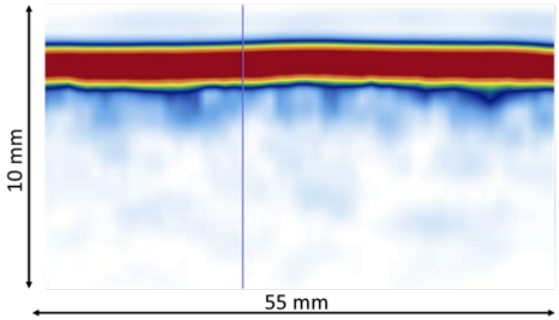

b)

Fig. 8. Comparisons of B-scan images obtained from composite samples for 20 x 20 mm defect at depth of: a)1 mm and b) 2 mm

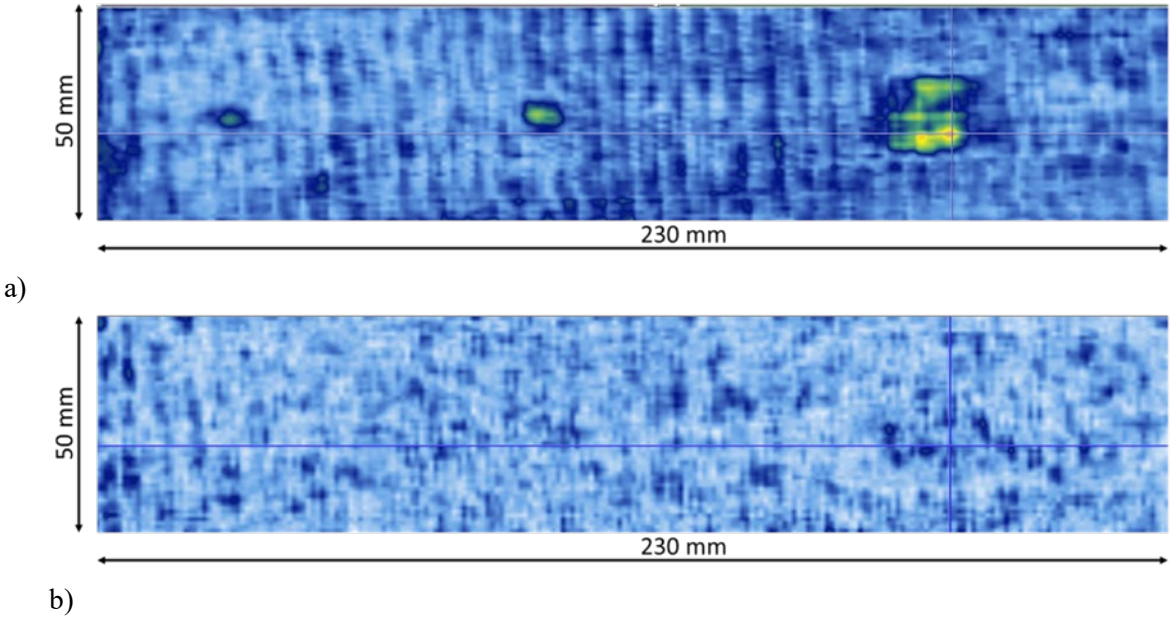

Fig. 9. Comparisons of C-scan images for all 3 defects, at depth of: a)1 mm and b) 2 mm

DISCUSSION

Composite structures manufactured by filament winding may contain characteristic defects such as gaps and overlaps between fibre tows, fibre waviness, dry spots, porosity, and interlaminar discontinuities formed during winding or curing. These flaws differ from the ideal planar PTFE inserts employed in the reference samples, but their acoustic behaviour can be related to the obtained SNR-based detectability map. Shallow interlaminar defects produce strong reflections similar to the inserts located at 1 mm and remain detectable with the proposed setup. In contrast, deeper matrix-related imperfections or fibre distribution irregularities generate weaker scattering signals and are expected to fall below the detectability threshold. Therefore, the proposed methodology provides a practical framework for assessing which classes of filament winding defects can be reliably identified in thin GFRP layers of tanks.

The presented PAUT approach is effective for detecting shallow planar defects, but its applicability is limited by the strong attenuation of ultrasonic waves in GFRP composites. As shown in both the simulations and experiments, defects located deeper than approximately 1–1.5 mm rapidly fall below the detection threshold, even when their size is relatively large. This restricts the method primarily to near-surface interlaminar discontinuities. Additionally, the structural noise associated with fibre architecture and microporosity can mask weak reflections, making small volumetric flaws difficult to identify.

Compared with other NDT methods used for composite tanks, PAUT plays a complementary role. Thermography and shearography are highly sensitive to surface disbonds but lack depth resolution. Radiography enables the detection of volumetric porosity but is less effective for planar defects and requires radiation safety measures. Acoustic emission is useful during pressurization tests but cannot map pre-existing manufacturing flaws. In this context, PAUT provides a depth-resolved, quantitative assessment of critical delamination-type defects in regions where other methods offer limited capability, making it a valuable addition to the inspection toolbox for filament wound type IV tanks.

CONCLUSIONS

Detecting flaws and defects in composite structures by means of NDT methods is widely used. The developed PAUT methodology demonstrated reliable detection of artificial delamination

in thin GFRP layers of type IV low-pressure composite tanks. The experimental determination of ultrasonic attenuation coefficients at 2, 4, and 5 MHz, followed by their implementation in CIVA simulations, confirmed the validity of the adopted numerical model. Both the simulation and experiment indicated that, at the centre frequency of 5 MHz, defects measuring 5 × 5 mm, 10 × 10 mm, and 20 × 20 mm were detectable only at depths up to approximately 1 mm, while deeper defects were below the detection threshold. The proposed SNR-based, color-coded detectability map (white – undetectable, yellow – limited detectability, green – optimal detectability) enables clear assessment of defect detectability. The combination of experimental measurements and numerical modelling provides a robust basis to further optimize PAUT inspection procedures for composite tanks.

Funding

The work presented in this paper was supported by the National Center for Research and Development in Poland, under project number MAZOWSZE/0141/19 entitled INNOTANK.

REFERENCES

[1] Chang, J., Zheng, Ch., Ni, Q-Q., The ultrasonic wave propagation in composite material and its characteristic evaluation, Composite Structures 75(1):451-456, 2006. DOI:10.1016/j.compstruct.2006.04.040

[2] Li, G., Neerukatti, R.K., Chattopadhyay, A., Ultrasonic guided wave propagation in composites including damage using high-fidelity local interaction simulation, Journal of Intelligent Material Systems and Structures, 29(5):969-985, 2017. DOI:10.1177/1045389X17730659

[3] Norouzian, M., Turner, J.A., Ultrasonic wave propagation predictions for polycrystalline materials using three-dimensional synthetic microstructures: Attenuation, The Journal of the Acoustical Society of America 145(4):2181-2191, 2019. DOI:10.1121/1.5096651

[4] Victoria-Giraldo, J.C. et al, Ultrasonic scattering in polycrystalline materials with elongated grains: A comparative 3D and 2D theoretical and numerical analysis, Ultrasonics 152 (2025) 107642. https://doi.org/10.1016/j.ultras.2025.107642

[5] Serrati, D.S.M.; Machado, M.A.; Oliveira, J.P.; Santos, T.G., Non-destructive testing inspection for metal components produced using wire and arc additive manufacturing, Metals 2023, 13, 648. https://doi.org/10.3390/met13040648

[6] Raišutis, R.; Kažys, R.; Mažeika, L.; Žukauskas, E.; Šliteris, R.; Vladišauskas, A. Application of ultrasonic guided waves for non-destructive testing of large and complex geometry engineering structures. Vibroengineering PROCEDIA 2017, 14, 87–90.

[7] Van Pamel, A.; Huthwaite, P.; Brett, C.R.; Lowe, M.J. Numerical simulations of ultrasonic array imaging of highly scattering materials. NDT E Int. 2016, 81, 9–19.

[8] Rosado, L.S.; Santos, T.G.; Piedade, M.; Ramos, P.M.; Vilaça, P. Advanced technique for non-destructive testing of friction stir welding of metals. Meas. J. Int. Meas. Confed. 2010, 43, 1021–1030

[9] Oliveira, T.L.L.; Hadded, M.; Mimouni, S.; Schaan, R.B. The Role of Non-Destructive Testing of Composite Materials for Aerospace Applications. NDT 2025, 3, 3. https://doi.org/10.3390/ndt3010003

[10] Rahman, M.S.U., Hassan, O.S., Mustapha, A.A., Abou-Khousa, M.A., & Cantwell, W.J. (2023). Inspection of thick composites: A comparative study between microwaves, X-ray computed tomography and ultrasonic testing. Nondestructive Testing and Evaluation, 1–18. https://doi.org/10.1080/10589759.2023.2287071

[11] Caminero, M.A., García-Moreno, I., Rodríguez, G.P., Chacón, J.M.. Internal damage evaluation of composite structures using phased array ultrasonic technique: Impact damage assessment in CFRP and 3D printed reinforced composites, Composites Part B: Engineering, (2019), 165, 131–142. https://doi.org/10.1016/j.compositesb.2018.11.091

[12] Garnier C., Pastor M.L., Eyma, F., Lorrain, B. The detection of aeronautical defects in situ on composite structures using non-destructive testing. Compos Struct, 93 (2011), pp. 1328–1336. DOI:10.1016/j.compstruct.2010.10.017

[13] Haridas, A., Song, C., Chan, K., Murukeshan, V.M.. Non-destructive characterization of thermal damages and its interactions in carbon fibre composite panels. Fatig Fract Eng Mater Struct, 40 (2017), pp. 1562–1580. https://doi.org/10.1111/ffe.12657

[14] Taheri, H.; Hassen, A.A. Nondestructive Ultrasonic Inspection of Composite Materials: A Comparative Advantage of Phased Array Ultrasonic. Appl. Sci. 2019, 9, 1628. https://doi.org/10.3390/app9081628

